Robustness of Retrospective Cost Adaptive Control to Markov-Parameter Uncertainty

E. Dogan Sumer, Anthony M. D'Amato, Alexey V. Morozov[1], Jesse B. Hoagg[2], and Dennis S. Bernstein[3]

***Abstract*— In this paper we investigate the robustness of an extended version of retrospective cost adaptive control (RCAC), in which less modeling information is required than in prior versions of this method. RCAC is applicable to MIMO possibly nonminimum-phase (NMP) plants without the need to know the locations of the NMP zeros. The only required modeling information is an FIR approximation of the plant, which may be based on a limited number of Markov parameters. In this paper we investigate the effect of phase mismatch between the true plant and the FIR approximation. Numerical examples demonstrate the relationship between phase mismatch at the command and disturbance frequencies as well as the required level of regularization in the controller update.**

I. Introduction

One of the motivations for adaptive control is the desire to minimize the amount of required modeling information [1–4]. For example, if an adaptive controller requires no knowledge of the plant pole locations, then it is unconditionally robust to the actual pole locations, assuming that they are constant or, perhaps, slowly changing. Since an adaptive controller is robust to modeling information that it does not need, an adaptive controller can be viewed as a robust nonlinear controller. Since an adaptive controller tunes itself to the actual plant, the main benefit of adaptive control is thus the reduced need to model the system for controller tuning without sacrificing performance.

Although model-free adaptive control allows arbitrary plant uncertainty, model-free control may entail large learning transients and may be subject to restrictions on zero locations [5]. Therefore, adaptive controllers typically rely on some plant modeling data, which is obtained through either prior modeling and identification or on-line identification.

In the present paper we focus on retrospective cost adaptive control (RCAC) [6–10]. In the SISO case, this approach relies on knowledge of the first nonzero Markov parameter and knowledge of the nonminimum-phase (NMP) zeros, if any; in the MIMO case, the number of Markov parameters that must be known depends on whether the plant is square, tall, or wide, as well as on the rank of the Markov parameters. Markov parameters provide a convenient foundation for plant modeling since they are independent of the state space basis, and they can be identified by various system identification methods [11]. When a sufficient number of Markov parameters are used within RCAC, the locations of the NMP zeros are approximately captured, which avoids the need to determine a state space realization and compute the NMP zeros.

In [12], RCAC is extended to remove the need to know the NMP zeros, as well as to reduce the number of required Markov parameters. In particular, it is shown in [12] that in many cases, a single nonzero Markov parameter suffices to achieve convergence of the adaptive controller.

The purpose of the present paper is to investigate the robustness implications of the accuracy and number of the Markov parameters used in RCAC. We thus consider SISO command following and disturbance rejection problems for open-loop-stable plants with sinusoidal commands and disturbances. In particular, we focus on the mismatch between the plant and the finite-impulse-response (FIR) approximation constructed from the chosen set of Markov parameters. Here, mismatch refers to the difference between the phase angle of the true plant and its FIR approximation constructed from the chosen Markov parameters when both transfer functions are evaluated on the unit circle. The numerical examples that we present demonstrate the phase mismatch that can be tolerated when the adaptive regularization term in the optimization step is appropriately chosen. Although FIR approximation of IIR plants is a longstanding problem in systems theory [13, 14], the challenge within the context of RCAC is to construct a suitable FIR approximation of the plant using minimal modeling information.

In Section 2 we present the adaptive control problem. Next, Section 3 shows that knowledge of the gain and phase of the plant at the frequency of the exogenous sinusoid is sufficient to guarantee convergence. Next, in Sections 4–6, we return to the Markov parameter formulation in Section 2, and we show how the phase mismatch depends on the choice and accuracy of the Markov parameters. In Section 5 we present numerical examples to demonstrate the performance of RCAC under various levels of phase mismatch. The role of adaptive regularization in the presence of large phase mismatch is also discussed.

[1]Graduate Student, Department of Aerospace Engineering, The University of Michigan

[2]Professor, Department of Mechanical Engineering, The University of Kentucky, Lexington, KY 40506-0503, jhoagg@engr.uky.edu

[3]Professor, Department of Aerospace Engineering, The University of Michigan, Ann Arbor, MI 48109-2140, dsbaero@umich.edu

II. Problem Formulation

Consider the MIMO discrete-time system

$$x(k+1) = Ax(k) + Bu(k) + D_1 w(k), \tag{1}$$

$$y(k) = Cx(k) + D_2 w(k), \tag{2}$$

$$z(k) = E_1 x(k) + E_0 w(k), \tag{3}$$

where $x(k) \in \mathbb{R}^n$, $y(k) \in \mathbb{R}^{l_y}$, $z(k) \in \mathbb{R}^{l_z}$, $u(k) \in \mathbb{R}^{l_u}$, $w(k) \in \mathbb{R}^{l_w}$, and $k \geq 0$. The open-loop system (1)–(3) is described by

$$\left[\begin{array}{c} z \\ y \end{array}\right] = G(z) \left[\begin{array}{c} w \\ u \end{array}\right],$$

where

$$G(z) = \left[\begin{array}{cc} G_{zw}(z) & G_{zu}(z) \\ G_{yw}(z) & G_{yu}(z) \end{array}\right].$$

Consider the LTI output feedback controller

$$x_{\rm c}(k+1) = A_{\rm c} x_{\rm c}(k) + B_{\rm c} y(k), \tag{4}$$

$$u(k) = C_{\rm c} x_{\rm c}(k), \tag{5}$$

where $x_{\rm c}(k) \in \mathbb{R}^{n_{\rm c}}$. The closed-loop system with output feedback (4)–(5) is thus given by

$$\tilde{x}(k+1) = \tilde{A}\tilde{x}(k) + \tilde{D}_1 w(k), \tag{6}$$

$$y(k) = \tilde{C}\tilde{x}(k) + D_2 w(k), \tag{7}$$

$$z(k) = \tilde{E}_1 \tilde{x}(k) + E_0 w(k), \tag{8}$$

where

$$\tilde{A} = \left[\begin{array}{cc} A & BC_{\rm c} \\ B_{\rm c}C & A_{\rm c} \end{array}\right], \tilde{D}_1 = \left[\begin{array}{c} D_1 \\ B_{\rm c}D_2 \end{array}\right],$$

$$\tilde{C} = \left[\begin{array}{cc} C & 0_{l_y \times n_{\rm c}} \end{array}\right], \tilde{E}_1 = \left[\begin{array}{cc} E_1 & 0_{l_z \times n_{\rm c}} \end{array}\right],$$

and $\tilde{x}(k) = \left[\begin{array}{cc} x^{\rm T}(k) & x_{\rm c}^{\rm T}(k) \end{array}\right]^{\rm T}$.

The goal is to develop an adaptive output feedback controller that minimizes the performance variable z in the presence of the exogenous signal w with limited modeling information about G. The components of the signal w can represent either command signals to be followed, external disturbances to be rejected, or both, depending on the configurations of D_1 and E_0.

For the adaptive system, $A_{\rm c} = A_{\rm c}(k)$, $B_{\rm c} = B_{\rm c}(k)$, and $C_{\rm c} = C_{\rm c}(k)$ are time varying, and (6)–(8) illustrates the structure of the time-varying closed-loop system in which $\tilde{A} = \tilde{A}(k)$. To monitor the ability of the adaptive controller to stabilize (1)–(3), we compute the spectral radius ${\rm spr}(\tilde{A}(k))$ of $\tilde{A}(k)$ at each time step. If ${\rm spr}(\tilde{A}(k))$ converges to a number less than 1, then the asymptotic closed-loop system is internally stable.

A detailed description of the Retrospective-Cost Adaptive Control algorithm is given in [12].

III. Finite-Impulse-Response Phase Matching

The RCAC algorithm described in [12] is based on Markov parameters of G_{zu} that are chosen by the user to construct the coefficient matrix $\tilde{\mathcal{H}}$. However, to illustrate the effect of these parameters on the performance of RCAC, we replace the Markov parameters of G_{zu} with constants κ_i. These constants can be viewed as either approximations to the Markov parameters or as parameters obtained by phase matching as explained below.

For $0 < j_1 < j_2 < \cdots < j_r$, and $\kappa_{j_r} \neq 0$, we define the $j_r^{\rm th}$-order FIR transfer function

$$G_{\rm FIR}(z) \triangleq \frac{\kappa_{j_1} z^{(j_r - j_1)} + \kappa_{j_2} z^{(j_r - j_2)} + \cdots + \kappa_{j_r}}{z^{j_r}}.$$

Next, for $\theta \in [0, \pi]$, the phase mismatch function $\Delta(\theta)$ between $G_{\rm FIR}$ and G_{zu} is defined by

$$\Delta(\theta) \triangleq \cos^{-1} \frac{{\rm Re}\left[G_{zu}(e^{\jmath\theta})\overline{G_{\rm FIR}(e^{\jmath\theta})}\right]}{|G_{zu}(e^{\jmath\theta})|\,|G_{\rm FIR}(e^{\jmath\theta})|} \in [0, 180]. \tag{9}$$

To illustrate the effect of phase matching, consider the $2^{\rm nd}$-order minimum-phase system $G_{zu}(z) = \frac{z-0.5}{(z-0.5+0.4\jmath)(z-0.5-0.4\jmath)}$. We consider the sinusoidal command $w(k) = \sin(\theta_0 k)$, where $\theta_0 = 1$ rad/sample. We assume that θ_0 and $G_{zu}(e^{\jmath\theta_0})$ are known. Then, taking $r = 2$, $j_1 = 1$, and $j_2 = 2$, we construct the second-order FIR model

$$G_{\rm FIR}(z) = \frac{\kappa_1 z + \kappa_2}{z^2},$$

where κ_1 and κ_2 are chosen so that $\Delta(\theta_0) = 0$. For this example, κ_1 and κ_2 are given by $\kappa_1 = 0.8792$, $\kappa_2 = 0.864$. The phase mismatch function illustrated in Figure 1 confirms that $G_{\rm FIR}$ exactly matches G_{zu} at $\theta_0 = 1$ rad/sample. Note that the Markov parameters H_1, H_2 of G_{zu} are $H_1 = 1$ and $H_2 = 0.5$, and thus κ_1 and κ_2 are not Markov parameters of $G_{zu}(z)$. We let $\tilde{\mathcal{H}} = \left[\begin{array}{cc} \kappa_2 & \kappa_1 \end{array}\right]^{\rm T}$, $n_{\rm c} = 5$, $\eta_0 = 0$, and $P_0 = I_{2n_{\rm c}}$. The performance $z(k)$ converges to zero, and the closed-loop system with the converged control gains $\theta(k)$ is stable as shown in Figure 2.

We now modify $\tilde{\mathcal{H}}$ by keeping κ_2 the same, but replacing $\kappa_1 = 0.8792$ by $\kappa_1 = -0.1792$. This modification increases the phase mismatch at θ_0 to $\Delta(1) = 40$ deg. Keeping the same controller parameters, we consider the same command $w(k) = \sin(k)$. The performance converges to zero and the closed-loop system is stable.

We now further decrease κ_1 to -0.8792 and keep κ_2 the same, so that the phase mismatch $\Delta(1)$ increases to 91 deg. Keeping the same controller parameters $n_{\rm c}$, P_0, and η_0, RCAC converges to an internal model controller with high gain at $\theta_0 = 1$ rad/sample, but destabilizes the system and thus cannot track the command, as shown in Figure 3.

Keeping κ_1, κ_2 the same so that $\Delta(1) = 91$ deg, we now introduce adaptive regularization by letting $\eta_0 = 0.1$. Keeping the same controller parameters $n_{\rm c}$ and P_0, the performance converges to zero, and adaptive regularization prevents RCAC from destabilizing the closed-loop system, as shown in Figure 4.

These numerical results indicate that phase matching plays

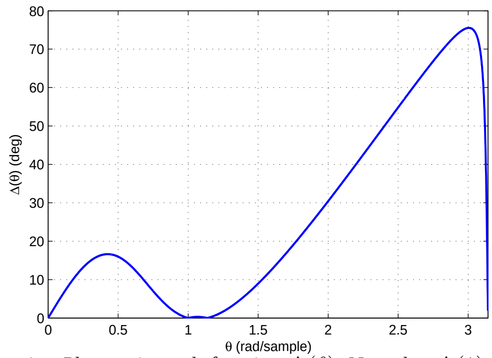

Fig. 1. Phase mismatch function $\Delta(\theta)$. Note that $\Delta(1) = 0$.

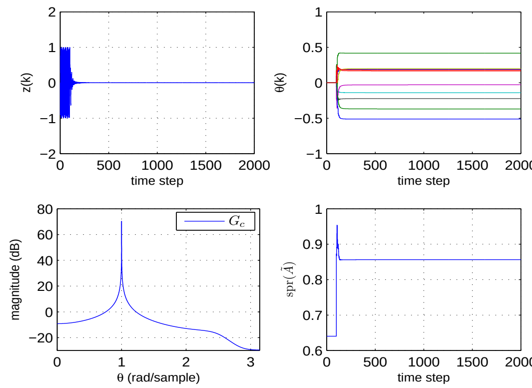

Fig. 2. Command following with $w(k) = \sin(k)$. In this case, $\tilde{\mathcal{H}}$ is constructed such that $\Delta(1) = 0$ deg, without using Markov parameters. The performance $z(k)$ converges to zero, and RCAC converges to an internal model controller with high gain at $\theta = 1$ rad/sample.

a role in the convergence of the performance and closed-loop stability. In practice, however, G_{zu} may be uncertain, and, furthermore, we may not know the frequency content of the exogenous input $w(k)$. In this case, we cannot construct $G_{\rm FIR}$ to match G_{zu} at the command or disturbance frequencies. We thus consider Markov-parameter-based constructions of $G_{\rm FIR}$.

IV. Markov Parameters and Phase Matching

Now, we return to the case in which $G_{\rm FIR}$ is constructed based on Markov parameters. For $0 < j_1 < j_2 < \cdots < j_r$, $H_{j_r} \neq 0$, consider the FIR approximation $G_{\rm FIR}(z)$ of $G_{zu}(z)$ given by

$$G_{\rm FIR}(z) = \frac{H_{j_1} z^{(j_r - j_1)} + H_{j_2} z^{(j_r - j_2)} + \cdots + H_{j_r}}{z^{j_r}},$$

where H_{j_i} are the Markov parameters of $G_{zu}(z)$. Note that $G_{\rm FIR}(z)$ approximates $G_{zu}(z)$ in the sense that the $j_i{}^{\rm th}$ Markov parameter H_{j_i} of $G_{zu}(z)$ is also the $j_i{}^{\rm th}$ Markov parameter of $G_{\rm FIR}(z)$ for $1 \le i \le r$. For $\theta \in [0, \pi]$, the phase mismatch function $\Delta(\theta)$ between $G_{\rm FIR}$ and G_{zu} is defined as in (9).

Different choices of Markov parameters H_{j_i} lead to different FIR models that have different levels of phase mismatch. For example, for the $2^{\rm nd}$-order nonminimum-phase system $G_{zu}(z) = \frac{z-1.5}{(z-0.8)(z-0.5)}$, taking $r = 1$, $j_1 = 1$ leads to the

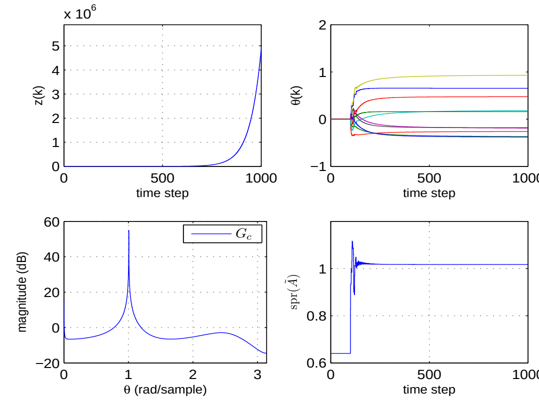

Fig. 3. Command following with $w(k) = \sin(k)$. In this case, $\tilde{\mathcal{H}}$ is constructed such that $\Delta(1) = 91$ deg, without using Markov parameters. The performance grows unbounded, and RCAC converges to a destabilizing internal model controller.

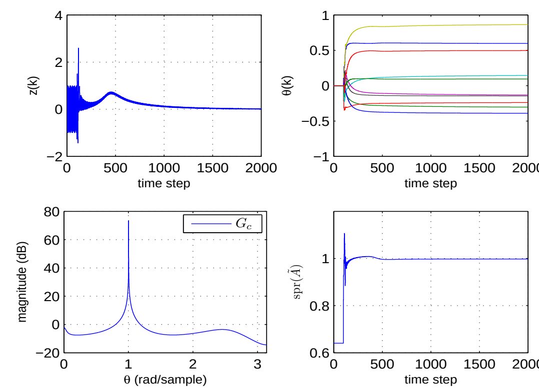

Fig. 4. Command following with $w(k) = \sin(k)$. In this case, $\tilde{\mathcal{H}}$ is constructed such that $\Delta(1) = 91$ deg, without using Markov parameters. In this case, adaptive regularization prevents RCAC from destabilizing the closed-loop system, and the performance $z(k)$ converges to zero.

$1^{\rm st}$-order FIR approximation

$$G_{\rm FIR}(z) = \frac{H_1}{z} = \frac{1}{z}. \tag{10}$$

Similarly, taking $r = 1$, and $j_1 = 2$ leads to the $2^{\rm nd}$-order FIR approximation

$$G_{\rm FIR}(z) = \frac{H_2}{z^2} = \frac{-0.2}{z^2}. \tag{11}$$

Figure 5 shows that the phase mismatch functions $\Delta_1(\theta)$ and $\Delta_2(\theta)$ corresponding to (10) and (11), respectively, are significantly different.

In general, using successively more Markov parameters in

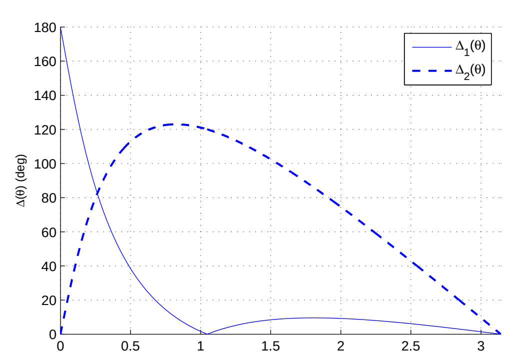

Fig. 5. Phase mismatch functions Δ_1 and Δ_2 for (10) and (11), respectively.

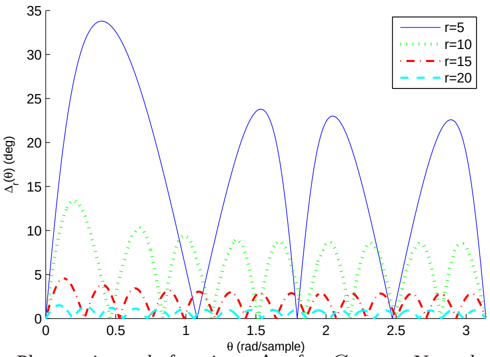

Fig. 6. Phase mismatch functions Δ_r for $G_{\mathrm{FIR},r}$. Note that the peak value of the phase mismatch decreases as r increases.

the construction of G_{FIR} leads to improved phase matching over $\theta \in [0, \pi]$. For example, for $G_{zu}(z)$ as defined above, define

$$G_{\mathrm{FIR},r}(z) \triangleq \sum_{i=1}^{r} \frac{H_i}{z^i} = \frac{H_1 z^{r-1} + \cdots + H_r}{z^r}$$

as the r^{th}-order FIR approximation with $j_i = i$, $1 \le i \le r$. Figure 6 shows that the peak of the phase mismatch function decreases as r increases. Note that phase matching matters only at the command and disturbance frequencies, which may or may not be known in practice. Furthermore, in addition to the number and choice of Markov parameters, the phase mismatch depends on the accuracy of the Markov parameters, as determined by the modeling accuracy.

The numerical results in the next section show that the level of regularization required for convergence of the adaptive controller depends on the phase mismatch at the command and disturbance frequencies. In particular, for command and disturbance frequencies at which the phase mismatch is less than 90 deg, RCAC is insensitive to the level of regularization. As the phase mismatch increases above 90 deg, the controller becomes more dependent on the choice of regularization η_0.

V. Command Following and Disturbance Rejection with Deterministic Signals

In this section, we present numerical examples to investigate the effect of the choice of $\tilde{\mathcal{H}}$ on the convergence of the adaptive controller. We consider the exogenous signal $w(k)$ generated by

$$x_w(k+1) = A_w x_w(k),$$
$$w(k) = C_w x_w(k),$$

where $x_w \in \mathbb{R}^{n_w}$, and A_w has distinct eigenvalues on the unit circle. Assuming that no command frequency is a zero of G_{zu}, and none of the eigenvalues $e^{\jmath\theta_i}$ of A_w are zeros of $G_{\mathrm{FIR}}(z)$, we show by numerical examples that a sufficient condition for convergence of z to zero is to have $\Delta(\theta_i) < 90$ deg for all $1 \le i \le n_w$ in the presence of adaptive regularization. When this condition is not satisfied, convergence may still be possible but may require an appropriate level of regularization.

Example 5.1: Consider the 2^{nd}-order plant $G_{zu}(z) = \frac{z-1.5}{(z-0.8)(z-0.5)}$. We consider a command following problem with the step command $w(k) = 2$. We first take $\tilde{\mathcal{H}} = H_1$, so that $\Delta(0) = 180$, as shown in Figure 5. We take $n_c = 3$, $P_0 = I_{2n_c}$, and $\eta_0 = 0.5$. The performance does not converge to zero, as shown in Figure 7. In fact, we observe that the performance is driven in the opposite direction due to the 180-deg phase mismatch at DC. We now take $\tilde{\mathcal{H}} = H_2$, so that $\Delta(0) = 0$, as shown in Figure 5. Keeping n_c, η_0, and P_0 the same, the performance now converges to zero, as shown in Figure 8. ■

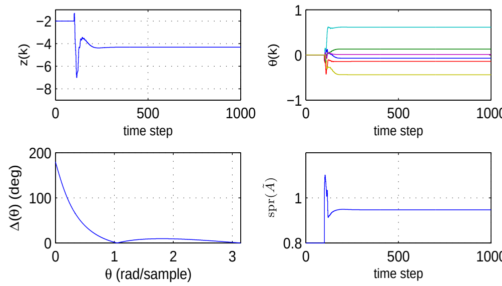

Fig. 7. Example 5.1: Stable, nonminimum-phase plant, step-command following. In this case, $\tilde{\mathcal{H}} = H_1$, so that $\Delta(0) = 180$ deg. The performance is driven in the wrong direction due to 180-deg phase mismatch at DC.

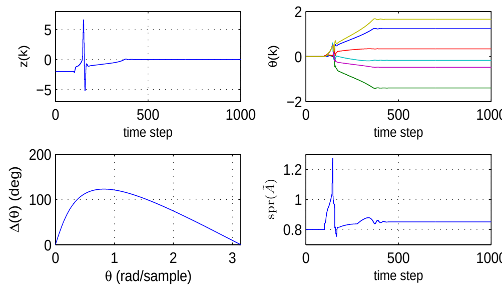

Fig. 8. Example 5.1: Stable, nonminimum-phase plant, step-command following. In this case, $\tilde{\mathcal{H}} = H_2$, so that $\Delta(0) = 0$ deg. The performance $z(k)$ now converges to zero.

Example 5.2: Consider 4^{th}-order plant $G_{zu}(z) = \frac{z(z-4)(z-3)}{(z-0.8)(z-0.6)(z-0.5-0.5\jmath)(z-0.5+0.5\jmath)}$. Taking $\tilde{\mathcal{H}} = H_1$, the phase mismatch function $\Delta(\theta)$ is illustrated in Figure 9.

We first consider the sinusoidal command $w(k) = \sin(\theta_0 k)$, where $\theta_0 = 2$ rad/sample. Figure 9 shows that $\Delta(2) = 2.3$ deg. We take $n_c = 6$, $P_0 = I_{2n_c}$, and vary η_0 from 0.01 to 10. Figure 10 shows that the performance $z(k)$ converges to zero for each choice of η_0, although the transient behavior is affected by the choice of η_0.

We now consider the sinusoidal command $w(k) =$

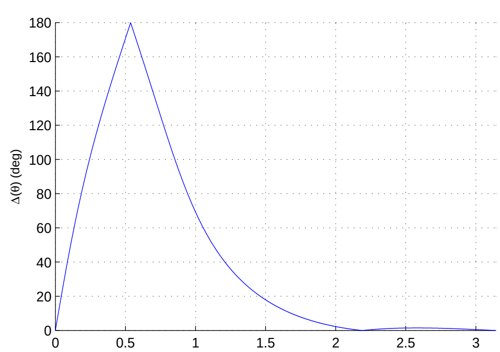

Fig. 9. Example 5.2: Phase mismatch function $\Delta(\theta)$ with $\tilde{\mathcal{H}} = H_1$.

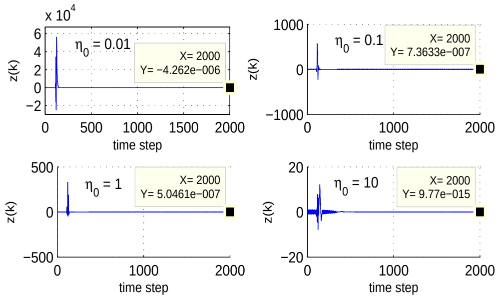

Fig. 10. Example 5.2: Stable, nonminimum-phase plant, command following with $w(k) = \sin(2k)$. Each subplot corresponds to a run with different η_0. The performance $z(k)$ converges to zero in each case, and the transient performance is improved as η_0 increases.

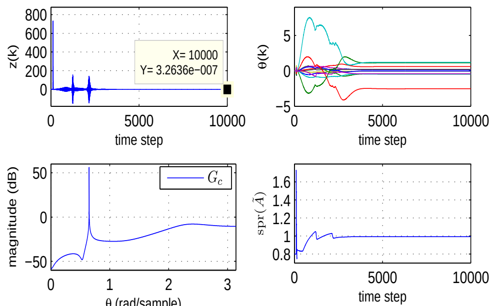

Fig. 11. Example 5.2: Stable, nonminimum-phase plant, command following with $w(k) = \sin(0.65k)$, $\eta_0 = 0.055$. The performance $z(k)$ converges to zero with this level of regularization even in the presence of large phase mismatch $\Delta(0.65) = 152$ deg at the command frequency. However, the large phase mismatch results in longer adaptation period.

$\sin(\theta_0 k)$, where $\theta_0 = 0.65$ rad/sample. Figure 9 shows that $G_{\rm FIR}$ does not match G_{zu} well at $\theta_0 = 0.65$ rad/sample with a phase mismatch $\Delta(0.65) = 152$ deg. We take $n_{\rm c} = 6$, $P_0 = I_{2n_{\rm c}}$, and vary η_0 from 0.01 to 10 as before. For all of the values of η_0, the performance $z(k)$ does not converge to zero.

Now, we consider the same command $w(k) = \sin(0.65k)$, and we take $n_{\rm c} = 6$ and $P_0 = I_{2n_{\rm c}}$, and $\eta_0 = 0.055$. The closed-loop response in Figure 11 shows that, with this level of regularization, the controller converges to a stabilizing internal model controller, and the performance $z(k)$ converges to zero. ∎

Example 5.3: Consider the 3rd-order plant $G_{zu}(z) = \frac{(z-1.8)(z-0.8)}{(z-0.85)(z-0.75-0.4\jmath)(z-0.75+0.4\jmath)}$. We consider the sinusoidal disturbance $w(k) = \sin(\theta_0 k)$, where $\theta_0 = 2.31$ rad/sample. With the plant realized in controllable canonical form, that is, $B = [\,1\ 0\ 0\,]^{\rm T}$, we take $D_1 = [\,0\ 1\ 0\,]^{\rm T}$, so that the disturbance is not matched with the input.

We first take $\tilde{\mathcal{H}} = H_1$, so that $\Delta(2.31) = 13$ deg. Taking $n_{\rm c} = 5$, $P_0 = 0.1 I_{2n_{\rm c}}$, and $\eta_0 = 1$, the closed-loop response in Figure 12 shows that the output $z(k)$ of the plant converges to zero, and RCAC converges to a stabilizing internal model controller.

We now take $\tilde{\mathcal{H}} = [\,H_4\ H_3\ H_2\ H_1\,]^{\rm T}$. Note that $\Delta(2.31) = 4.5$ deg, however, $G_{\rm FIR}$ has a zero at the disturbance frequency $e^{\jmath\theta_0}$. Taking $n_{\rm c} = 5$, $P_0 = 0.1 I_{2n_{\rm c}}$, and $\eta_0 = 1$, the closed-loop response in Figure 13 shows that, due to the zero of $G_{\rm FIR}$ at the disturbance frequency, RCAC does not adapt, and thus the controller gains remain at zero. Consequently,

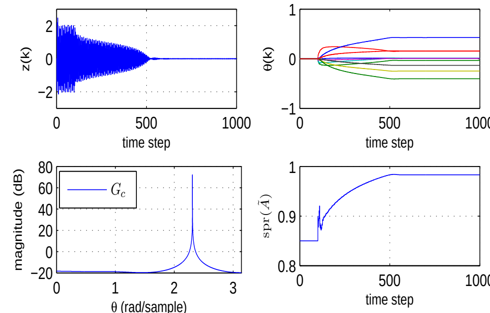

Fig. 12. Example 5.3: Stable, nonminimum-phase plant, unmatched disturbance rejection with $w(k) = \sin(2.31k)$. In this case, $\tilde{\mathcal{H}} = H_1$, so that $\Delta(2.31) = 13$ deg. The performance $z(k)$ converges to zero.

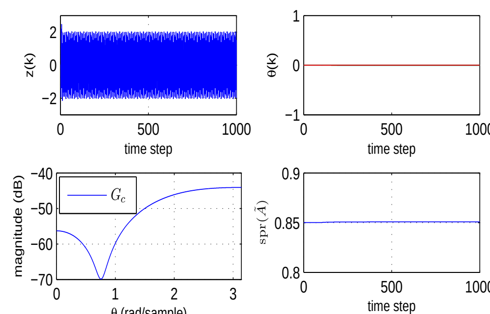

Fig. 13. Example 5.3: Stable, nonminimum-phase plant, unmatched disturbance rejection with $w(k) = \sin(2.31k)$. In this case, $\Delta(2.31) = 4.5$ deg, but RCAC cannot adapt since $G_{\rm FIR}$ has zeros at the disturbance frequency $e^{\pm\jmath\theta_0}$.

the adaptive controller cannot affect the performance. ∎

Example 5.4: We consider the plant G_{zu} in Example 5.3. With the plant realized in controllable canonical form, we take $E_0 = [\,0\ 0\ 0\ {-1}\ {-1}\ {-1}\,]$, $D_1 = [\,I_{3\times3}\ 0_{3\times3}\,]$, and consider the exogenous signal $w(k) = [\,w_1(k)\ \cdots\ w_6(k)\,]^{\rm T} = [\,\sin\theta_1\ \cdots\ \sin\theta_6\,]^{\rm T}$, where the disturbance frequencies are $\theta_1 = 0.6$ rad/sample, $\theta_2 = 1.2$ rad/sample, $\theta_3 = 1.8$ rad/sample, and the command frequencies are $\theta_4 = 0$ rad/sample, $\theta_5 = 2.4$ rad/sample, and $\theta_6 = 3$ rad/sample.

We first take $\tilde{\mathcal{H}} = H_1$, which yields $\Delta_1(\theta)$ shown in Figure 14. Taking $n_{\rm c} = 25$, $P_0 = 0.1 I_{2n_{\rm c}}$, and $\eta_0 = 0.1$, the performance $z(k)$ does not converge to zero because of the large phase mismatch at low frequencies.

Now taking $\tilde{\mathcal{H}} = [\,H_3\ H_2\ H_1\,]^{\rm T}$ yields $\Delta_3(\theta)$ shown in Figure 14. Taking $n_{\rm c} = 25$, $P_0 = 0.1 I_{2n_{\rm c}}$, and $\eta_0 = 0.1$, the closed-loop response illustrated in Figure 15 shows that the performance $z(k)$ converges to zero. ∎

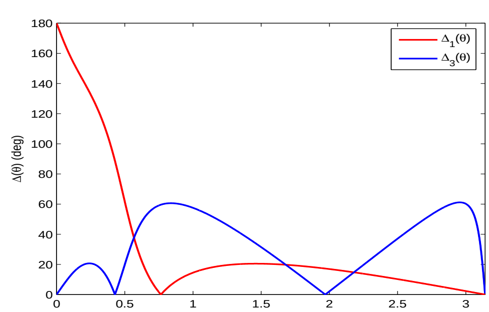

Fig. 14. Example 5.4: Phase mismatch functions Δ_1 and Δ_3.

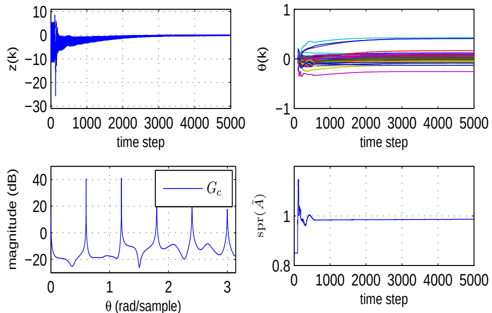

Fig. 15. Example 5.4: Command following and disturbance rejection with a 6-tone exogenous signal. In this case, $\Delta_3(\theta) < 90$ deg for all $0 \leq \theta \leq \pi$, and the performance $z(k)$ converges to zero.

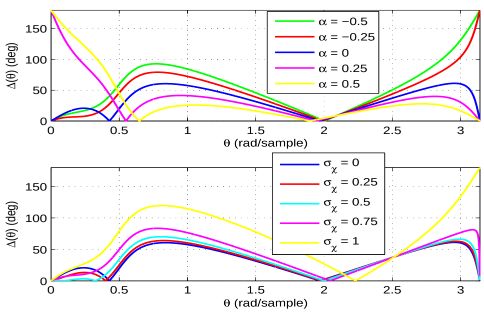

Fig. 16. This figure shows the effect of uniform additive error and random additive error in the Markov parameters for the plant in Example 5.4, and $r = 3$. For positive α, degradation is highest at $\theta = 0$, whereas, for negative α, degradation is highest at $\theta = \pi$. Degradation is low at the intermediate frequencies for all α. With $\sigma_\chi = 1$, $\Delta(\pi) = 180$ deg, and degradation is lower at all other angles.

VI. Robustness to Uncertain Markov Parameters

We now investigate robustness of RCAC when the Markov parameters are not known perfectly. We consider two types of uncertainty. For each type, we investigate the degradation in phase matching as the uncertainty level increases.

For $r \geq 1$, $H_r \neq 0$, we define the uniform additive uncertainty α, and random additive uncertainty $\sigma_\chi > 0$ such that

$$\tilde{\mathcal{H}} = \left[\begin{array}{ccc} H_r + \alpha & \cdots & H_1 + \alpha \end{array} \right]^{\mathrm{T}},$$
$$\tilde{\mathcal{H}} = \left[\begin{array}{ccc} H_r & \cdots & H_1 \end{array} \right]^{\mathrm{T}} + \chi(0, \sigma_\chi),$$

where H_i are the Markov parameters of $G_{zu}(z)$, α is a constant, and $\chi(0, \sigma_\chi) \in \mathbb{R}^r$ is a normally distributed random vector with zero mean and covariance $\sigma_\chi^2 I_r$.

For $r \geq 2$, uniform additive uncertainty and random additive uncertainty can introduce 180-deg phase mismatch at DC or the Nyquist frequency. In Figure 16, we show the effect of uniform and random additive uncertainty for the plant in Example 5.4, and $r = 3$, $\tilde{\mathcal{H}} = \left[H_3 \; H_2 \; H_1 \right] = \left[-1.145 \; -0.25 \; 1 \right]$. Positive α brings $\Delta(0)$ to 180 deg for $\alpha = 0.25 H_1$ and $\alpha = 0.5 H_1$, while negative α brings $\Delta(\pi)$ to 180 deg for $\alpha = -0.25 H_1$ and $\alpha = -0.5 H_1$. Note that degradation at intermediate frequencies is lower compared to $\theta = 0$ and $\theta = \pi$, for both positive and negative α. Furthermore, $\Delta(\pi)$ degrades to 180 deg for $\sigma_\chi = 1 H_1$, although lower frequencies are less affected compared to $\theta = \pi$.

VII. Conclusions

We provided a numerical investigation of the performance and robustness of retrospective cost adaptive control (RCAC). In particular, we considered the effect of the choice and accuracy of the Markov parameters used by RCAC. For the case in which the plant is known at the frequency of the command and disturbance signals, we showed that, if parameters of an FIR model are chosen to match the phase of the plant, then RCAC stabilizes the plant with an internal model that achieves command following and disturbance rejection. In this case, the only information needed about the plant is a single point on its Nyquist plot. For the case in which the plant or spectrum of the exogenous signals may be unknown, we considered the effect of the choice of Markov parameters, and we showed that the phase difference between the plant and the FIR model constructed from the Markov parameters determines the level of adaptive regularization needed for convergence. Finally, we considered the phase mismatch due to uncertainty in the Markov parameters.

References

[1] K. J. Astrom and B. Wittenmark, *Adaptive Control*, 2nd ed., Addison-Wesley, 1995.

[2] G. C. Goodwin and K. S. Sin, *Adaptive Filtering, Prediction and Control*, Prentice Hall, 1984.

[3] P. A. Ioannou, and J. Sun, *Robust Adaptive Control*, Prentice Hall, 1996.

[4] G. Tao, *Adaptive Control Design and Analysis*, Wiley, 2003.

[5] A. Ilchmann, *Non-Identifier-Based High-Gain Adaptive Control*, Springer-Verlag, 1993.

[6] R. Venugopal and D. S. Bernstein. “Adaptive Disturbance Rejection Using ARMARKOV System Representations,” *IEEE Trans. Contr. Sys. Tech.*, Vol. 8, pp. 257–269, 2000.

[7] J. B. Hoagg, M. A. Santillo, and D. S. Bernstein, “Discrete-Time Adaptive Command Following and Disturbance Rejection for Minimum Phase Systems with Unknown Exogenous Dynamics,” *IEEE Trans. Autom. Contr.*, Vol. 53, pp. 912–928, 2008.

[8] M. A. Santillo and D. S. Bernstein, “Adaptive Control Based on Retrospective Cost Optimization,” *AIAA J. Guid. Contr. Dyn.*, Vol. 33, pp. 289–304, 2010.

[9] J. B. Hoagg and D. S. Bernstein, ”Retrospective Cost Adaptive Control for Nonminimum-Phase Discrete-Time Systems Part 1: The Ideal Controller and Error System, Part 2: The Adaptive Controller and Stability Analysis,” *Proc. Conf. Dec. Contr.*, pp. 893–904, Atlanta, GA, December 2010.

[10] J. B. Hoagg and D. S. Bernstein, “Retrospective Cost Model Reference Adaptive Control for Nonminimum-Phase Discrete-Time Systems, Part 1: The Ideal Controller and Error System; Part 2: The Adaptive Controller and Stability Analysis,” *Proc. Amer. Contr. Conf.*, pp. 2927–2938, San Francisco, CA, June 2011.

[11] M. S. Fledderjohn, M. S. Holzel, H. Palanthandalam-Madapusi, R. J. Fuentes and D. S. Bernstein, ”A Comparison of Least Squares Algorithms for Estimating Markov Parameters”, *Proc. Amer. Contr. Conf.*, pp. 3735–3740, Baltimore, MD, June 2010.

[12] A. M. D’Amato, E. D. Sumer, and D. S. Bernstein, “Retrospective Cost Adaptive Control for Systems with Unknown Nonminimum-phase Zeros,” *Proc. Conf. Dec. Contr.*, Orlando, FL, December 2011.

[13] L. Chai, J. Zhang, C. Zhang, and E. Mosca , “From IIR to FIR Digital MIMO Models: A Constructive Hankel Norm Approximation Method,” *Proc. Conf. Dec. Contr.*, pp. 5893–5898, Seville, Spain, December 2005.

[14] Y. Yamamato, B. D. O. Anderson, M. Nagahara, and Y. Koyanagi, “Optimizing FIR Approximation for Discrete-Time IIR Filters,” *IEEE Signal Processing Letters*, vol. 10, no. 9, pp. 273-276, September 2003.